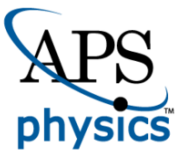

Two-Flavor QCD Correction to Lepton Magnetic Moments at Leading Order in the Electromagnetic Coupling

Xu Feng, Karl Jansen, Marcus Petschlies, and Dru B. Renner

Phys. Rev. Lett. **107**, 081802 — Published 17 August 2011

DOI: 10.1103/PhysRevLett.107.081802

Two-flavor QCD correction to lepton magnetic moments at leading-order in the electromagnetic coupling

Xu Feng,[1,2,*] Karl Jansen,[1] Marcus Petschlies,[3] and Dru B. Renner[1,†]
(ETMC Collaboration)

[1] *NIC, DESY, Platanenallee 6, D-15738 Zeuthen, Germany*
[2] *Universität Münster, Institut für Theoretische Physik, Wilhelm-Klemm-Strasse 9, D-48149, Germany*
[3] *Institut für Physik, Humboldt-Universität zu Berlin, D-12489, Berlin, Germany*

We present a reliable nonperturbative calculation of the QCD correction, at leading-order in the electromagnetic coupling, to the anomalous magnetic moment of the electron, muon and tau leptons using two-flavor lattice QCD. We use multiple lattice spacings, multiple volumes and a broad range of quark masses to control the continuum, infinite-volume and chiral limits. We examine the impact of the commonly ignored disconnected diagrams and introduce a modification to the previously used method that results in a well-controlled lattice calculation. We obtain $1.513\,(43)\cdot 10^{-12}$, $5.72\,(16)\cdot 10^{-8}$ and $2.650\,(54)\cdot 10^{-6}$ for the leading-order two-flavor QCD correction to the anomalous magnetic moment of the electron, muon and tau respectively, each accurate to better than 3%.

PACS numbers: 14.60.Ef, 12.38.Gc
Keywords: lepton anomalous magnetic moments, hadronic vacuum polarization, lattice QCD

INTRODUCTION

The experimental [1] and theoretical [2] determinations of the anomalous magnetic moment of the muon a_μ have both reached an accuracy that is better than six parts-per-million. This high precision reveals a discrepancy of over three standard deviations (3σ), which raises the possibility of physics beyond the Standard Model. However, the dominant error in the theory computation is due to hadronic effects that are currently not calculated but are instead either separately measured or simply modeled. This obscures the significance of the 3σ effect and makes it difficult to improve the accuracy of the Standard Model calculation.

In this Letter, we present a reliable lattice QCD determination of the leading-order hadronic correction for the muon, $a_\mu^{\rm hvp}$, which is the single largest source of error in the theory calculation of a_μ. Additionally, we calculate the leading-order corrections $a_e^{\rm hvp}$ for the electron and $a_\tau^{\rm hvp}$ for the tau, achieving an accuracy of better than 3% for each. This was accomplished by introducing a modification of the existing method that results in a significantly more well-controlled calculation. After examining all sources of systematic error and performing our own extraction of the two-flavor contribution to the experimental measurements, we find agreement for all three charged leptons in the Standard Model.

Our current computation is performed in two-flavor QCD, but the technique presented in this work is readily generalized to a realistic four-flavor calculation that is already underway [3]. The precision of our calculation and the prospects for improving it demonstrate that lattice QCD can realistically provide a first-principles determination of the leading-order hadronic contributions to the magnetic moments of the Standard Model leptons.

LEADING-ORDER HADRONIC CORRECTION

The anomalous magnetic moment a_l of a lepton l can be written as a perturbative expansion in the electromagnetic coupling α. Contributions from QCD first occur at the order α^2 and can be written as [4]

$$a_l^{\rm hvp} = \alpha^2 \int_0^\infty dQ^2 \frac{1}{Q^2} w(Q^2/m_l^2)\, \Pi_R(Q^2)\,, \qquad (1)$$

where m_l is the mass of the lepton, Q is the Euclidean momentum and $w(Q^2/m_l^2)$ is a known function. The combination $\Pi_R(Q^2) = \Pi(Q^2) - \Pi(0)$ is the renormalized hadronic vacuum polarization function $\Pi(Q^2)$, which is defined shortly. The weight function $w(Q^2/m_l^2)$ vanishes as $(Q^2)^{-2}$ for large Q^2. This ensures that the integral above is dominated by the low Q^2 region, making it clear that $a_l^{\rm hvp}$ must be evaluated nonperturbatively.

EXPERIMENTAL DETERMINATION

The electron and muon magnetic moments have been measured in dedicated experiments [1, 5]. To compare to the Standard Model prediction, the leading-order hadronic correction is determined by using unitarity and causality to relate the expression in Eq. 1 to

$$a_l^{\rm hvp} = \alpha^2 \int_0^\infty ds \frac{1}{s} w'(s/m_l^2)\, R(s)\,. \qquad (2)$$

Here w' is another known weight function and $R(s)$ is the ratio of the hadronic cross-section $\sigma(e^+e^- \to \text{hadrons})$ to the leptonic cross-section $\sigma(e^+e^- \to \mu^+\mu^-)$. The determination of $R(s)$ relies on the results of many experiments, and the integral in Eq. 2 has been evaluated by several groups, most recently [2, 6–8]. Additionally, there

are higher-order corrections, including the so-called light-by-light contribution, which is difficult to measure and is modeled instead.

Our calculation is performed in QCD with only up and down quarks, so we need to extract the two-flavor contribution to $a_l^{\rm hvp}$. Inevitably, this introduces some ambiguity. For the purposes of comparing to our current two-flavor calculation, we adopt the simple procedure of rescaling the contribution to the integral in Eq. 2 from the energy regions between quark thresholds by the value of $\sum_f Q_f^2$, where the sum runs over only the active quark flavors for that region and the electric charges of the quarks are eQ_f. This neglects the very small changes due to the running of the QCD coupling, it ignores small off-diagonal contributions proportional to $Q_f Q_{f'}$, and it disregards any complications at the flavor thresholds. These are all caveats that we must accept in the current comparisons but that will be eliminated in our ongoing four-flavor computation.

Using the results from [9, 10], we extract the two-flavor contributions to $a_l^{\rm hvp}$ along the lines just described, giving $a_{e,N_f=2}^{\rm hvp,ex} = 1.547\,(36)\cdot 10^{-12}$, $a_{\mu,N_f=2}^{\rm hvp,ex} = 5.660\,(47)\cdot 10^{-8}$ and $a_{\tau,N_f=2}^{\rm hvp,ex} = 2.638\,(88)\cdot 10^{-6}$. The errors result from propagating just those of [9, 10]. The systematic error due to extracting the two-flavor contribution is likely larger than these uncertainties and must be taken into consideration when comparing our calculation to these estimates.

LATTICE QCD CALCULATION

The leading-order hadronic correction, $a_l^{\rm hvp}$, is the order α^2 contribution in a perturbative QED expansion of a_l but it must be treated nonperturbatively in QCD. To this order in the QED coupling, the QCD corrections only modify the photon propagator. These contributions can be formally summed to all orders giving the hadronic vacuum polarization tensor,

$$\Pi_{\mu\nu}(Q) = \int d^4X\, e^{iQ\cdot X} \langle \Omega | T J_\mu(X) J_\nu(0) | \Omega \rangle \,.$$

The current $J_\mu = \sum_f Q_f \overline{q}_f \gamma_\mu q_f$ is the hadronic component of the electromagnetic current and the sum runs over all relevant quark flavors. The current J_μ is conserved, consequently this correlation function satisfies a Ward identity that allows us to write $\Pi_{\mu\nu}$ in terms of a single scalar function of Q^2 as

$$\Pi_{\mu\nu}(Q) = (Q_\mu Q_\nu - Q^2\delta_{\mu\nu})\Pi(Q^2)\,.$$

Note that both $\Pi_{\mu\nu}$ and Π are calculated directly in Euclidean space without any analytic continuation.

We use standard lattice QCD techniques to calculate the vacuum-to-vacuum matrix element $\langle \Omega | T J_\mu(x) J_\mu(y) | \Omega \rangle$. The functional integral that is implicit in this correlation function is evaluated stochastically using the results of the European Twisted Mass Collaboration [11]. We have used two lattice spacings, $a = 0.079$ and $a = 0.063$ fm, to examine lattice cutoff corrections. Two finite-volume studies were performed to check for finite-size effects. The up and down quark masses m_q are equal and are parameterized in terms of the pseudo-scalar meson mass m_{PS}, with $m_q \propto m_{PS}^2$ in the chiral limit. As is common, we use heavier-than-physical quark masses and then take the limit as m_{PS} approaches the physical pion mass m_π. This was done by studying the dependence on m_{PS} over the range from 650 to 290 MeV. The so-called disconnected diagrams, ignored in all previous calculations, were included for almost half of the ensembles used in this work and are accounted for as a systematic error along with those from the continuum, infinite-volume and physical quark-mass limits. The additional details are standard and deferred to a later publication.

Apart from variations in how the lattice calculation of $\Pi(Q^2)$ is matched to a smooth function, the method used so far in all calculations [4, 12–14] proceeds by numerically integrating Eq. 1 directly to form $a_l^{\rm hvp}$. In our calculation, we parameterize $\Pi(Q^2)$ over the entire range of Q^2 that is determined from our lattice computation. The presence of the lattice cutoff and the restriction to finite volume induce an ultraviolet cutoff $Q_{\rm uv}^2$ proportional to $1/a^2$ and an infrared cutoff proportional to $1/L^2$. Extrapolating the functional form for $\Pi(Q^2)$ to $Q^2 = 0$ [15], we numerically evaluate the integral from $Q^2 = 0$ to $Q^2 = Q_{\rm uv}^2$. This is done without any use of perturbation theory, giving a completely nonperturbative evaluation of $a_l^{\rm hvp}$. The systematic error caused by extrapolating to $Q^2 = 0$ is eliminated as L is taken large and the error due to truncating the integral at $Q_{\rm uv}^2$ is removed as a goes to zero. Thus both effects are automatically accounted for as part of the corresponding systematic errors.

Our results for the muon using this method, which we deem the *standard* method, are shown as the lowest set of points in Fig. 1. Consistent with all other lattice calculations of $a_\mu^{\rm hvp}$, we find that the values calculated at m_{PS} heavier than m_π are significantly lower than the experimentally measured value and apparently rise rapidly only when m_{PS} approaches quite near the physical value m_π.

We attribute this behavior to the contributions of the lowest-lying vector mesons. The rho, omega and phi mesons account for over 80% of the fully measured $a_\mu^{\rm hvp}$ [9]. Any description of the vector-meson contribution to $a_l^{\rm hvp}$ will depend on the mass m_V and a variety of dimensionless couplings. Without loss of generality, we focus on just those models based on m_V and the electromagnetic coupling g_V with $\langle \Omega | J_\mu | V, \epsilon \rangle = m_V^2 g_V \epsilon_\mu / \sqrt{2}$. The coupling shows up quadratically and dimensional analysis then results in a vector-meson contribution of

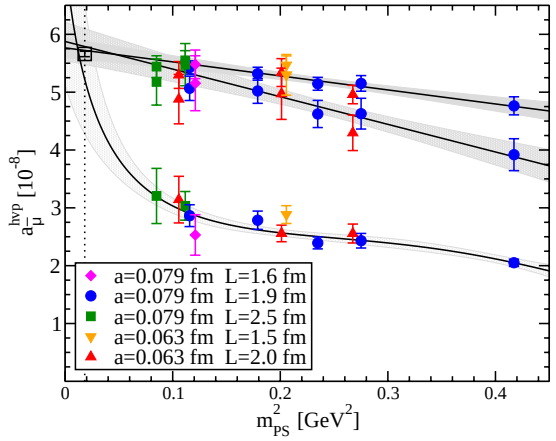

FIG. 1: Comparison of methods for $a_\mu^{\rm hvp}$. The upper set of points are the results for $a_{\bar{\mu}}^{\rm hvp}$ using $H = m_V$, the middle set use $H = f_V$ and the lower set correspond to the standard method, formally $H = 1$. The two lines are linear extrapolations of $a_{\bar{\mu}}^{\rm hvp}$ and the curve is the phenomenological extrapolation of $a_\mu^{\rm hvp}$. The three methods agree at the physical point, denoted by the dashed line, and agree with the estimated two-flavor contribution to the experimental value.

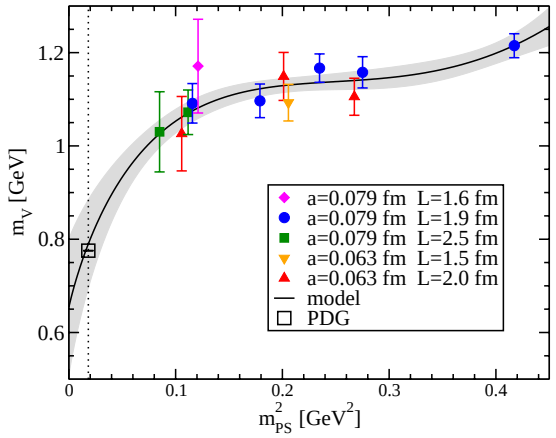

FIG. 2: Phenomenological model for m_V. A model function is used to parameterize both our lattice calculation of m_V and the PDG value of the physical m_ρ. This model is only used to illustrate the difficulties in the standard method.

$a_{l,V}^{\rm hvp} = g_V^2 f(m_l^2/m_V^2)$. Additionally, $f(m_l^2/m_V^2)$ should vanish for $m_l \to 0$ and $m_V \to \infty$. Thus on rather general grounds we expect $a_{l,V}^{\rm hvp} \approx C g_V^2 m_l^2/m_V^2$ with a model-dependent constant C.

These expectations can be combined with our lattice calculation of m_V and g_V. As shown in Fig. 2, we find that m_V decreases moderately with decreasing m_{PS} but the values from our calculation are still rather high compared to the experimental result m_ρ. Thus at some point a rapid decrease in m_V must occur. In contrast, g_V, not shown but well fit by $g_V = 0.29(1) - 0.09(2)\, m_{PS}^2$, has a mild dependence on m_{PS} and extrapolates smoothly to the experimental value g_ρ. When combined with the model expectation $a_{\mu,V}^{\rm hvp} \propto g_V^2/m_V^2$, the behavior of $a_\mu^{\rm hvp}$ in Fig. 1 becomes plausible. The values of $a_\mu^{\rm hvp}$ are lower than the experimental value and vary moderately for the region of m_{PS} covered in our calculation. Only at lighter values of m_{PS} do we expect a sharp increase in $a_\mu^{\rm hvp}$.

We can make these observations more precise, at the expense of introducing model dependence, by considering the tree-level form for the vector-meson contribution $a_{l,V}^{\rm hvp}$ as given from effective field theory [13]. This gives a specific result for $f(m_l^2/m_V^2)$ that we combine with our calculation of m_V and g_V to construct a model-dependent extrapolation of the results for $a_\mu^{\rm hvp}$. Additionally, constraining m_V to approach m_ρ as shown in Fig. 2 gives the lowest lying curve in Fig. 1. The apparent agreement with the physical value for $a_\mu^{\rm hvp}$ increases the plausibility that our explanation is correct. However, this construction does not provide a reliable means of extrapolating our results to the physical m_π but instead serves to illustrate the apparently strong m_{PS} dependence in the standard method.

The difficulties encountered in the standard method can be traced to the occurrence of two distinct scales, m_l and m_V. Apart from any model, this is relevant because $a_l^{\rm hvp}$ is made dimensionless at the expense of introducing an external scale m_l that is completely unrelated to the scales of QCD. Based on this observation, we define the following class of observables

$$a_{\bar{l}}^{\rm hvp} = \alpha^2 \int_0^\infty dQ^2 \frac{1}{Q^2} w(Q^2/m_l^2 \cdot H_{\rm phys}^2/H^2)\, \Pi_R(Q^2) \quad (3)$$

where H is any hadronic quantity, understood to be a function of m_{PS}, and $H_{\rm phys}$ is its physical value. The natural choice for our calculation is $H = m_V$, but any choice produces a new modified quantity that has the same physical limit as $a_l^{\rm hvp}$. This follows simply by construction because $H(m_{PS} \to m_\pi) = H_{\rm phys}$. The standard method can be formally reproduced by the choice $H = 1$, but choosing a dimensionful scale has the additional advantage that the explicit dependence on the lattice spacing is eliminated. At the same time, the renormalization condition that defines the physical limit is now given by the dimensionless ratio $m_l/H_{\rm phys}$ rather than m_l alone.

The calculation of $a_{\bar{\mu}}^{\rm hvp}$ using $H = m_V$ and $H = f_V$, the vector-meson decay constant given by $f_V = m_V g_V$, are shown in Fig. 1. All three extrapolations agree with each other and with the estimated two-flavor contribution to the experimental measurement of $a_\mu^{\rm hvp}$. The results for the new method show a significantly milder dependence on m_{PS}. This can be understood using the model considerations earlier. Specifically for $H = m_V$, we expect a vector-meson contribution of $a_{\bar{l},V} \approx C g_V^2 m_l^2/m_\rho^2$, in which only the mild m_{PS} dependence of g_V now enters. The demonstration that $H = f_V$ results in similar improvements illustrates that any quantity sensitive to m_V will likely yield a well-controlled observable $a_{\bar{l}}^{\rm hvp}$.

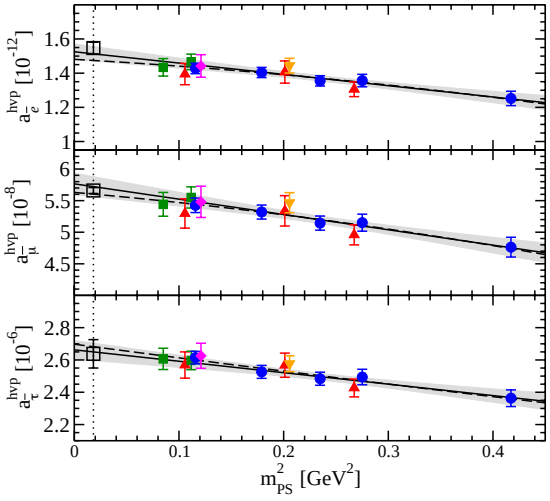

FIG. 3: Calculation of $a_{\bar{l}}^{\rm hvp}$ for all three $l = e$, μ and τ. The meaning of the symbols is the same as in Fig. 1. We show the results from our improved method using $H = m_V$. The results are extrapolated linearly (solid line with error band) and quadratically (dashed line) to the physical point and agree with the two-flavor contribution extracted from the experimental measurements.

Without regard to any particular model or the experimental measurements, we can examine the relative merits of the standard and modified methods. Using the muon as an example, the shift between linear and quadratic extrapolations for $a_{\bar{\mu}}^{\rm hvp}$ (using $H = m_V$) is 1.7%, which is only a $0.6\,\sigma$ effect. The same results for $a_\mu^{\rm hvp}$ are 17% and $3.5\,\sigma$, indicating the presence of noticeably more curvature in the standard approach. In this case, cubic fits are required and give an extrapolated value of $4.1\,(1.5)\cdot 10^{-8}$, which agrees with the more precise value of $5.72\,(16)\cdot 10^{-8}$ that results from extrapolating $a_{\bar{\mu}}^{\rm hvp}$. The same pattern holds for the electron and tau, thus the lattice calculation itself provides direct evidence that our modified method has a smoother approach to the physical limit leading to a more accurate calculation.

Taking the modified method with $H = m_V$ as our definition of $a_{\bar{l}}^{\rm hvp}$, we calculate all three $l = e$, μ and τ. These results are shown in Fig. 3, and the extrapolated values at the physical point are

$$\begin{aligned} a_{e,N_f=2}^{\rm hvp} &= 1.513\,(43)\cdot 10^{-12} \\ a_{\mu,N_f=2}^{\rm hvp} &= 5.72\,(16)\cdot 10^{-8} \\ a_{\tau,N_f=2}^{\rm hvp} &= 2.650\,(54)\cdot 10^{-6}\,. \end{aligned}$$

The quoted errors are due to the stochastic integration only. We do not find any statistically meaningful uncertainties due to lattice artifacts, finite-size effects, the extrapolation in m_{PS} or the exclusion of the disconnected diagrams. At some higher precision these effects will be relevant, but there is no sign that they are significant at the few percent level of our current calculation.

CONCLUSIONS AND OUTLOOK

We have performed the first lattice QCD calculation of the leading-order QCD correction to the anomalous magnetic moments, $a_l^{\rm hvp}$, that included dynamical quarks, examined lattice artifacts, checked finite-size effects and studied the disconnected diagrams. We examined the pitfalls of the standard method for calculating $a_l^{\rm hvp}$ and introduced a modification that creates a dimensionless quantity $a_{\bar{l}}^{\rm hvp}$ composed of hadronic scales only. This quantity has the same physical limit as $a_l^{\rm hvp}$ but has a mild approach to that limit that is now well controlled. This allowed us to calculate the leading-order correction for all three charged leptons with an accuracy better than 3%, reproducing our estimate of the two-flavor contributions to the experimental measurements.

The calculation was done using two-flavor QCD, which is the most significant systematic error. To resolve this, we are currently starting a four-flavor calculation. This will eliminate any ambiguity regarding the extraction of the two-flavor experimental value. When combined with further anticipated improvements, the modified method presented here should produce a result precise enough to replace the experimentally estimated $a_l^{\rm hvp}$ with a complete first-principles QCD calculation and eliminate this source of ambiguity in the current 3σ discrepancy in a_μ.

We thank our fellow members of ETMC for their constant collaboration. We are grateful to the John von Neumann Institute for Computing (NIC), the Jülich Supercomputing Center and the DESY Zeuthen Computing Center for their computing resources and support. This work has been supported in part by the DFG Sonderforschungsbereich/Transregio SFB/TR9-03, the DFG project Mu 757/13 and the U.S. DOE under Contract No. DE-AC05-06OR23177.

* Current address: KEK.
† Current address: Jefferson Lab.

[1] Muon G-2 Collaboration, Phys. Rev. **D73**, 072003 (2006).
[2] Jegerlehner and Nyffeler, Phys. Rept. **477**, 1 (2009).
[3] ETMC Collaboration, JHEP **1006**, 111 (2010).
[4] Blum, Phys. Rev. Lett. **91**, 052001 (2003).
[5] Hanneke *et al.*, Phys. Rev. Lett. **100**, 120801 (2008).
[6] Davier *et al.*, Eur. Phys. J. **C71**, 1515 (2011).
[7] Jegerlehner and Szafron, Eur. Phys. J. **C71**, 1632 (2011).
[8] Hagiwara *et al.*, (2011), arXiv:1105.3149.
[9] Jegerlehner, Nucl. Phys. Proc. Suppl. **181-182**, 26 (2008).
[10] Jegerlehner, Nucl. Phys. Proc. Suppl. **51C**, 131 (1996).
[11] ETMC Collaboration, JHEP **08**, 097 (2010).
[12] QCDSF Collaboration, Nucl. Phys. **B688**, 135 (2004).
[13] Aubin and Blum, Phys. Rev. **D75**, 114502 (2007).
[14] Brandt *et al.*, PoS **LAT2010** (2010).
[15] Renner *et al.*, PoS **ICHEP2010**, 371 (2010).